ARGOMENTI DI TESI

5.8 GHz FMCW RADAR

Radar MIMO 5.8 GHz

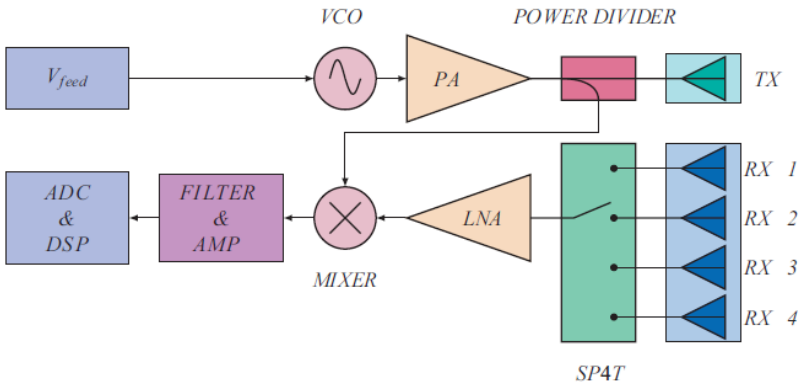

Figure 1: Typical architecture of FMCW radars.

Radar Realization

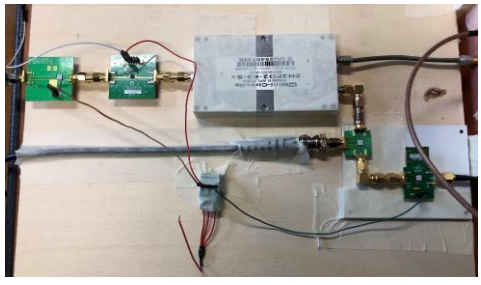

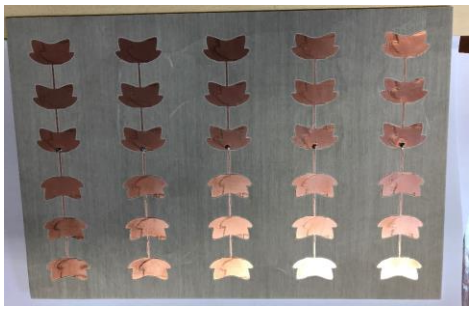

HMC587LC4B: VCO, Analog Devices.
HMC407MS8G: POWER AMPLIFIER, Analog Devices.
HMC344ALP3E: SWITCH SP4T, Analog Devices.
HMC392ALC4: LNA, Analog Devices.
HMC557A : MIXER, Analog Devices.

VSS (MWO)

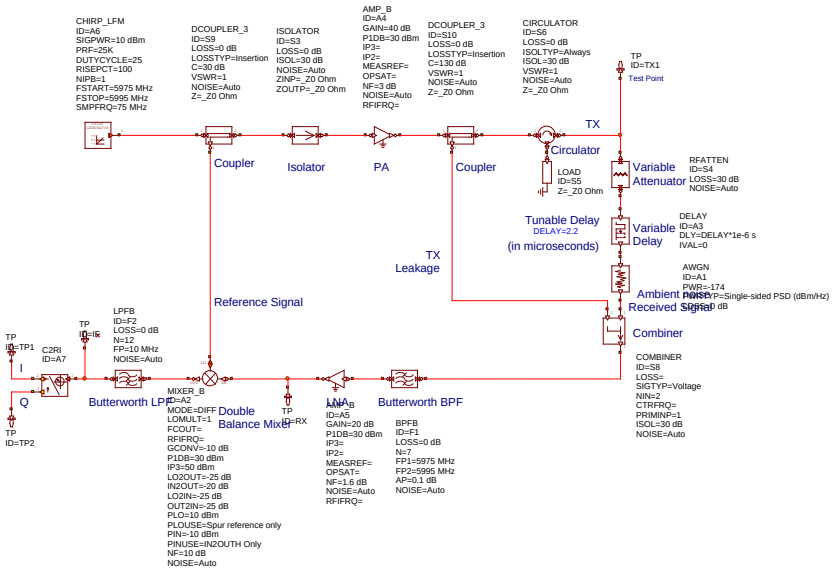

VSS Results

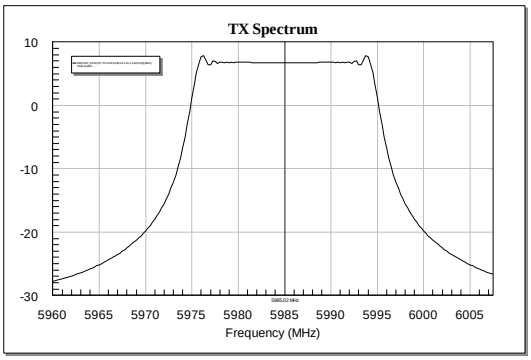

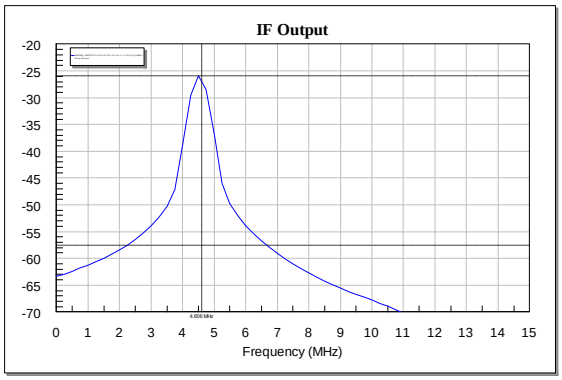

24 GHz FMCW RADAR

BGT24MTR11

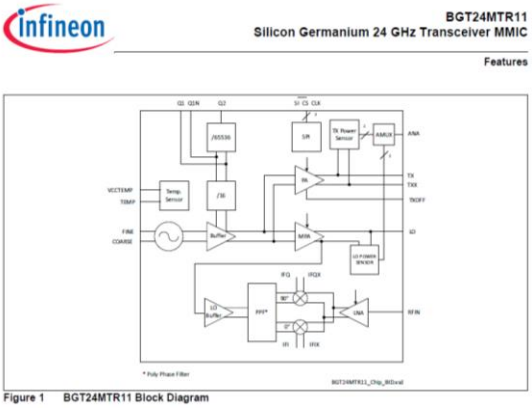

BGT24MTR11
Silicon Germanium 24 GHz Transceiver MMIC

Features

Figure 1 BGT24MTR11 Block Diagram

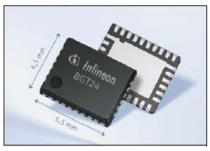

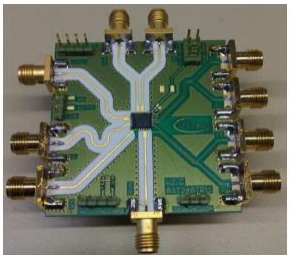

Acquisizione ed elaborazione segnale radar

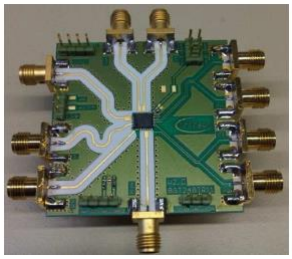

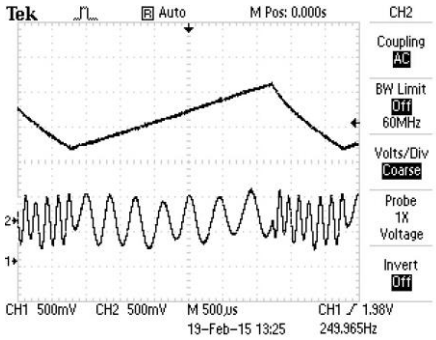

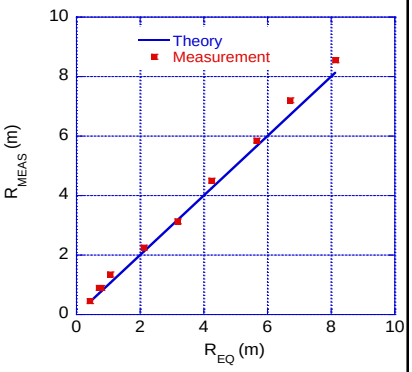

Campi di Applicazione

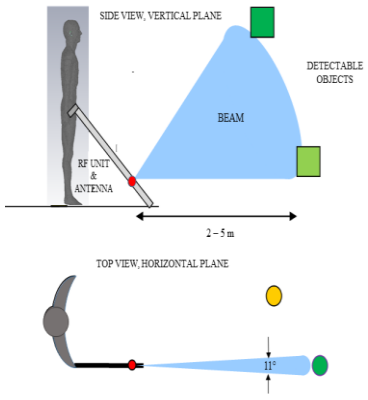

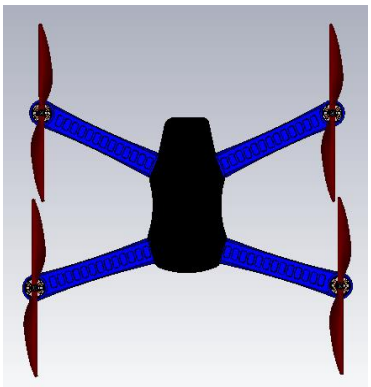

Integrated Devices

ADF4159 della **Analog Devices (**PLL)

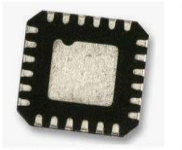

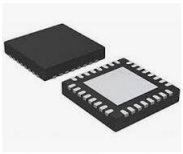

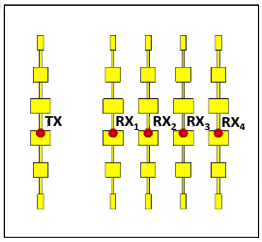

ADRF5045 dell'Analog Devices (switch)

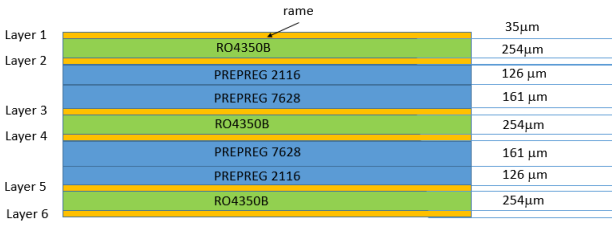

RF Board

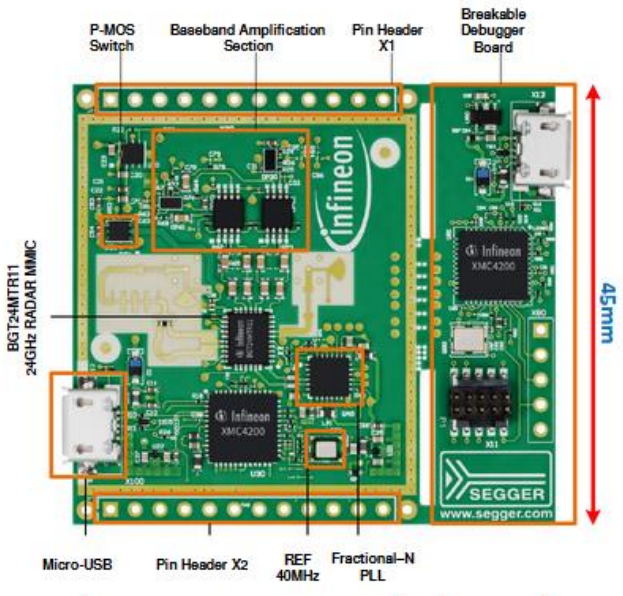

Altium Designer

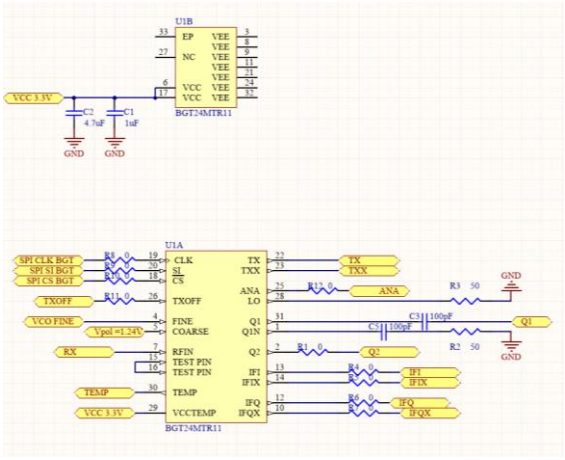

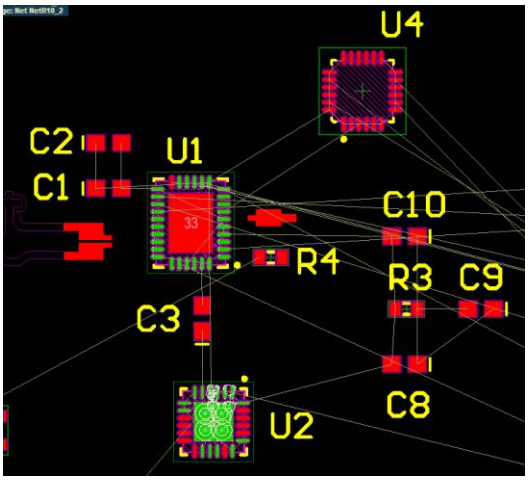

STEP FREQUENCY RADAR 1-3 GHz

Through The Wall radar Imaging

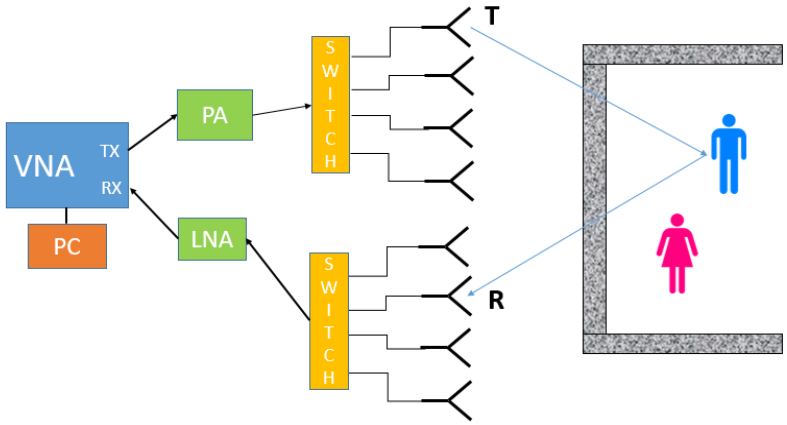

Inversion algorithms (Delay and Sum)

Pixel intensity

$$I(i,j) = \sum_{k=1}^{Npos} \sum_{l=1}^{Nfreq} \boldsymbol{S_{21}}(l) e^{j\frac{2\pi}{\lambda} d(k)} e^{j\frac{2\pi}{\lambda} \tau_D}$$

d(k) is the transmitting antenna-pixel-receiving antenna distance

τ_D is the delay between the excitation ports and the physical ones antenna

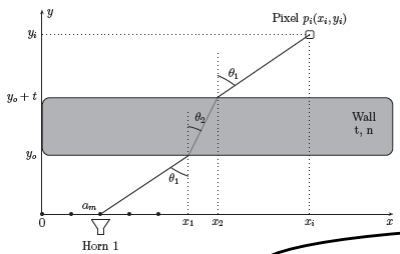

For taking into account the refraction caused by the wall the Fermat's principle can be implemented by minimising a function depending on the wall permittivity:

$$d(a_m, (x_i, y_i)) = \sqrt{(\hat{x}_1 - a_m)^2 + y_o^2} + n\sqrt{(\hat{x}_2 - \hat{x}_1)^2 + t^2} + \sqrt{(x_i - \hat{x}_2)^2 + (y - y_o - t)^2}$$

16 antennas, lambda/4 DAS Algorithm

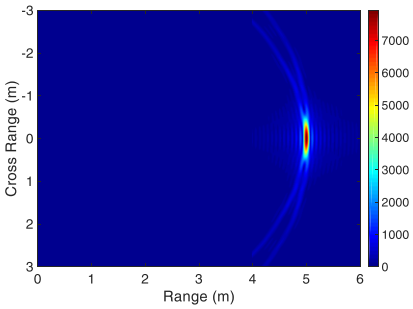

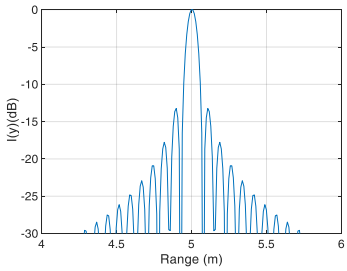

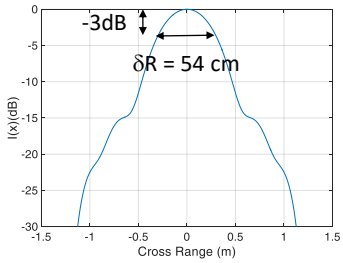

Experimental Set-Up

PNA E3683C

DAC

Pasternack

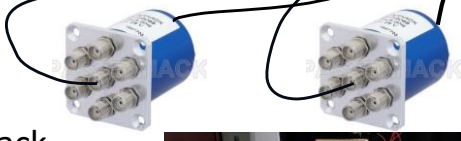

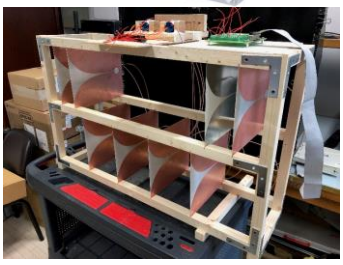

ANTENNAS

Experimental Result

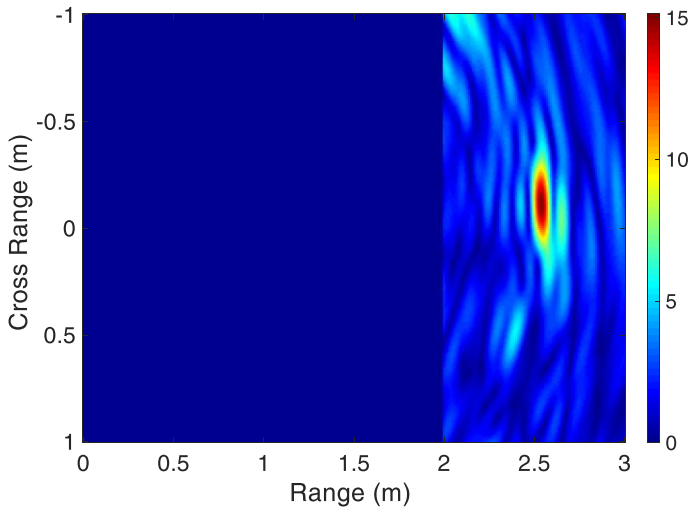

ELECTRON PARAMAGNETIC RESONANCE

Helmholtz coils were designed and the **modulation field homogeneity** was investigated.

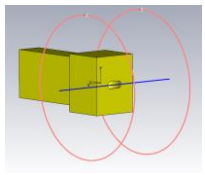

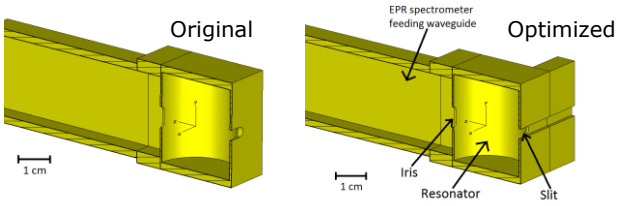

The structures were optimized.

Higher homogeneity was obtained.

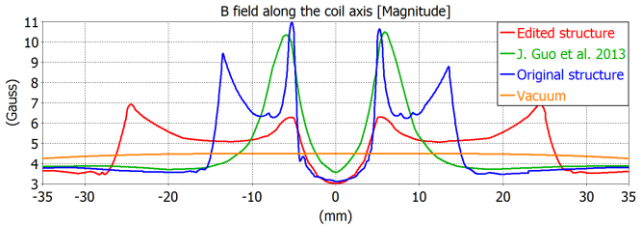

The structure was divided in **three different parts**:

The **resonator**

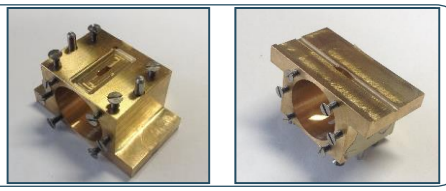

The **lid**

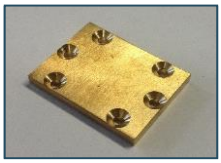

The **coupling unit**

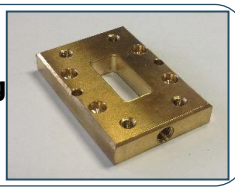

The cavity was manufactured in the mechanical workshop of the ISS, by mechanical specialists, using **pure brass** (instead of silver).

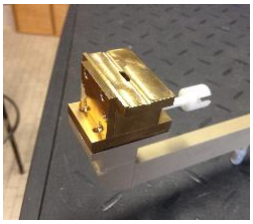

The cavity was tested using an **Agilent E8363C Precision Network Analyzer** (PNA)

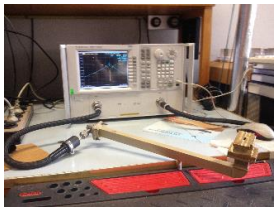

In order to estimate the losses introduced by the waveguide, a **fitting routine** was used.

Results obtained:

Data from	Tuning screw	f_0 (GHz)	Q_U	α	β
Simulation	No	9.575	5822	-	0.533
PNA	No	9.560	4266	-	0.46
Fit	No	9.560	4193	0.88	0.409
PNA	Yes	9.560	4146	-	1.00
Fit	Yes	9.560	4325	0.83	0.993

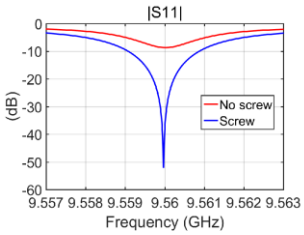

Measurements

The efficacy of the whole system was tested by using, as sample material, a powder of stable free-radical molecules (DPPH), positioned on an adhesive support in contact with the slit.
The figure shows the signal recorded by the bruker spectrometer equipped with the realised open resonator.

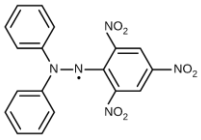

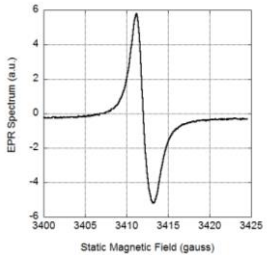

IMPEDENZIOMETRO MULTIFREQUENZA

Configurazione del sistema di misura

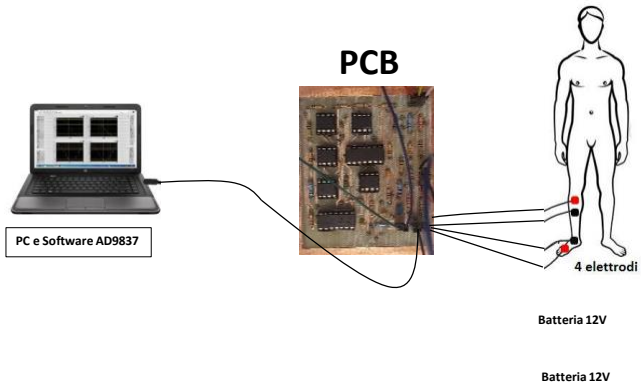

SCHEMATICO DEL CIRCUITO

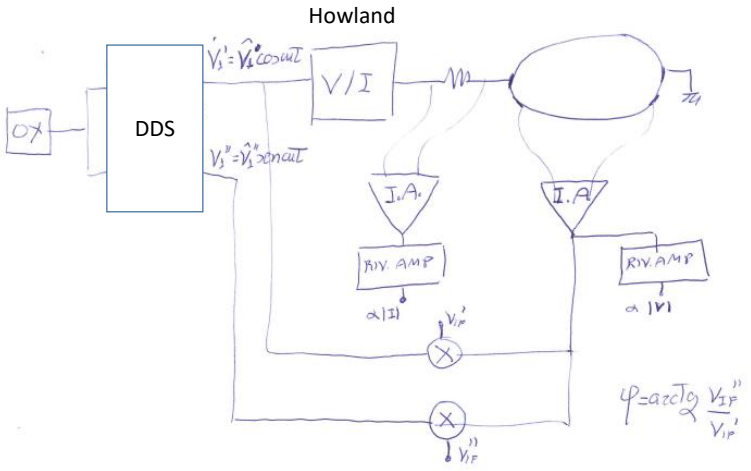

PULSE TRANSIT TIME

A

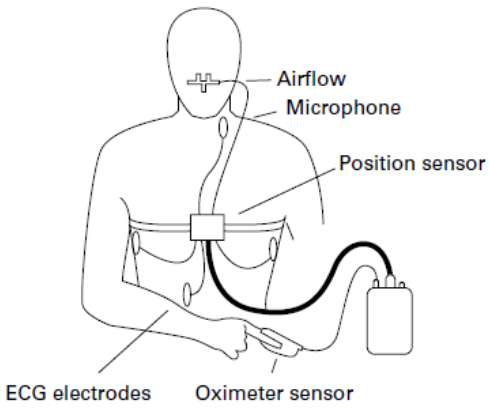

B

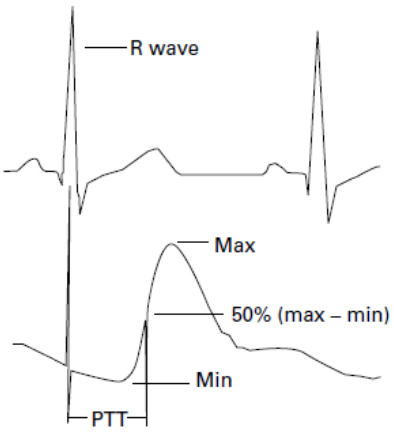

AFE4490 TEXAS INSTRUMENTS
PULSOSSSIMETRO

Olimex (ECG)